Journal of Experimental Botany, Vol. 74, No. 12 pp. 3579–3594, 2023
https://doi.org/10.1093/jxb/erad091 Advance Access Publication 13 March 2023
This paper is available online free of all access charges (see https://academic.oup.com/jxb/pages/openaccess for further details)

RESEARCH PAPER

Cytokinin signaling promotes root hair growth by directly regulating *RSL4* expression

Hirotomo Takatsuka[1,2], Anna Sasaki[1], Naoki Takahashi[1], Michitaro Shibata[3], Keiko Sugimoto[3,4], Maho Tanaka[3,5], Motoaki Seki[3,5] and Masaaki Umeda[1,*]

[1] Graduate School of Science and Technology, Nara Institute of Science and Technology, 8916-5 Takayama, Ikoma, Nara 630-0192, Japan
[2] School of Biological Science and Technology, College of Science and Engineering, Kanazawa University, Kakuma-machi, Kanazawa, Ishikawa 920-1192, Japan
[3] RIKEN Center for Sustainable Resource Science, Tsurumi-ku, Yokohama, Kanagawa 230-0045, Japan
[4] Department of Biological Sciences, The University of Tokyo, Tokyo, 119-0033, Japan
[5] RIKEN Cluster for Pioneering Research, 2-1 Hirosawa, Wako, Saitama 351-0198, Japan

[*] Correspondence: mumeda@bs.naist.jp

Received 6 March 2023; Editorial decision 2 March 2023; Accepted 9 March 2023

Editor: Daniel Gibbs, University of Birmingham, UK

Abstract

Root hairs are single-celled tubular structures produced from the epidermis, which play an essential role in water and nutrient uptake from the soil. Therefore, root hair formation and elongation are controlled not only by developmental programs but also by environmental factors, enabling plants to survive under fluctuating conditions. Phytohormones are key signals that link environmental cues to developmental programs; indeed, root hair elongation is known to be controlled by auxin and ethylene. Another phytohormone, cytokinin, also affects root hair growth, while whether cytokinin is actively involved in root hair growth and, if so, how it regulates the signaling pathway governing root hair development have remained unknown. In this study, we show that the two-component system of cytokinin, which involves the B-type response regulators ARABIDOPSIS RESPONSE REGULATOR 1 (ARR1) and ARR12, promotes the elongation process of root hairs. They directly up-regulate *ROOT HAIR DEFECTIVE 6-LIKE 4* (*RSL4*) encoding a basic helix–loop–helix (bHLH) transcription factor that plays a central role in root hair growth, whereas the ARR1/12–RSL4 pathway does not crosstalk with auxin or ethylene signaling. These results indicate that cytokinin signaling constitutes another input onto the regulatory module governed by RSL4, making it possible to fine-tune root hair growth in changing environments.

Keywords: ARABIDOPSIS HISTIDINE KINASE, *Arabidopsis thaliana*, B-type ARABIDOPSIS RESPONSE REGULATOR, cytokinin, root hair, ROOT HAIR DEFECTIVE 6-LIKE 4.

Introduction

In *Arabidopsis thaliana*, the root epidermis consists of two cell files, the trichoblast [hair (H)] and atrichoblast [non-hair (N)]. Epidermal cells in contact with two cortical cells acquire the H cell type and form root hairs. Those overlying one cortical

cell differentiate into N cells that never produce root hairs (Gilroy and Jones, 2000; Jones *et al.*, 2009; Schiefelbein *et al.*, 2009; Takatsuka and Ito, 2020). Since root hairs contribute to an increase in root surface area, they enhance the uptake of nutrients and water, promoting overall plant growth (Gilroy and Jones, 2000; Jones *et al.*, 2009). Indeed, plants with short root hairs yield less biomass under limited nutrient conditions (Bates and Lynch, 2000). Yi *et al.* (2010) reported that the basic helix–loop–helix (bHLH) transcription factor ROOT HAIR DEFECTIVE 6-LIKE 4 (RSL4) plays a vital role in root hair growth. The RSL4 protein starts to accumulate in H cells at the onset of hair elongation and disappears when the hair growth terminates. Knockout and overexpression lines of *RSL4* display shorter and longer hairs than the wild type, respectively, implying that RSL4 plays a decisive role in hair outgrowth. Its expression is directly regulated by another bHLH transcription factor ROOT HAIR DEFECTIVE 6 (RHD6); *RSL4* is scarcely expressed in the absence of *RHD6* and its close homolog *RSL1* (Yi *et al.*, 2010). The expression of *RSL4* is also under the control of phytohormones, such as auxin and ethylene (López-Bucio *et al.*, 2003; Guimil and Dunand, 2007; Ishida *et al.*, 2008; Yi *et al.*, 2010; Feng *et al.*, 2017). AUXIN RESPONSE FACTOR 5 (ARF5), ARF7, ARF8, and ARF19, which bind to the promoters of early auxin response genes, directly control *RSL4* expression, enabling the auxin-dependent induction of root hair growth (Mangano *et al.*, 2017). Moreover, ETHYLENE INSENSITIVE 3 (EIN3) and its homolog ETHYLENE INSENSITIVE 3-LIKE 1 (EIL1), which are key transcription factors for ethylene signaling, also bind to the *RSL4* promoter and up-regulate its expression (Feng *et al.*, 2017).

Whereas the role of auxin and ethylene in root hair growth has been thoroughly studied, the involvement of other hormones remains elusive. Previous studies have reported that exogenously applied cytokinin (CK) promotes the elongation of root hair and that the overexpression of *CYTOKININ OXIDASE 2* (*CKX2*), which encodes a key enzyme responsible for CK degradation, results in the formation of short root hairs, suggesting a promoting function of CK in root hair growth (Su and Howell, 1992; An *et al.*, 2012; Zhang *et al.*, 2016). Although, according to the transcriptomic data, several root hair-related genes, including *RSL4*, were up-regulated by CK treatment, whether such transcriptional induction is indeed associated with root hair elongation remains elusive (Zhang *et al.*, 2016). CK is one of the major hormones governing developmental programs and mediating external signals; for instance, drought stress induces *CKX* and reduces CK levels and signaling (Le *et al.*, 2012). Therefore, understanding how CK controls root hair growth will provide clues to figure out plant strategies for coping with fluctuating environmental conditions.

CK controls a wide spectrum of biological processes by activating the two-component system called the 'phosphorelay'. In Arabidopsis, CK is perceived by the histidine kinase receptors ARABIDOPSIS HISTIDINE KINASE 2 (AHK2), AHK3, and AHK4, and the phosphate group is transmitted to the histidine phosphotransfer proteins (HPTs) and then to B-type ARABIDOPSIS RESPONSE REGULATORs (ARRs) (Inoue *et al.*, 2001; To and Kieber, 2008; Hwang *et al.*, 2012). The activated B-type ARRs function as transcription factors that induce the expression of CK-responsive genes (Sakai *et al.*, 2001; To *et al.*, 2004; Mason *et al.*, 2004; To and Kieber, 2008). In Arabidopsis roots, CK promotes cell differentiation, which in turn reduces the meristem size. At the boundary between the meristematic zone and the transition zone, B-type ARRs, ARR1 and ARR12, directly up-regulate the expression of *SHORT HYPOCOTYL 2* (*SHY2*) and inhibit auxin signaling by repressing *PIN-FORMED* (*PIN*) genes that encode auxin efflux carriers (Dello Ioio et al., 2007, 2008). Simultaneously, another B-type ARR, ARR2, induces *CELL CYCLE SWITCH 52A1* (*CCS52A1*) and activates the anaphase-promoting complex/cyclosome (APC/C), a multisubunit E3 ubiquitin ligase that functions in degrading mitotic cyclins (Takahashi *et al.*, 2013). Because of this, cell division stops, and endoreplication and cell differentiation proceed, leading to cell elongation. CK is also engaged in the second mode of cell elongation; namely, the AHK3/4–ARR2 pathway regulates actin dynamics to trigger more rapid cell elongation (Takatsuka *et al.*, 2018). Despite such accumulating information on the role of CK in the control of cell division, cell differentiation, and cell elongation, thus far the components of CK signaling involved in root hair growth remain unknown.

Here we report that CK promotes root hair elongation through the two-component system involving the B-type ARRs, ARR1 and ARR12. Additionally, we found that *RSL4* is directly induced by ARR1, thereby playing a crucial role in CK-dependent root hair growth, while ethylene and auxin are not associated with this process.

Materials and methods

Plant materials and growth conditions

Arabidopsis thaliana (ecotype Col-0) was grown vertically on Murashige and Skoog (MS) plates [1× MS salts, 0.5 g l^{-1} MES, 1× MS vitamin solution, 1% sucrose, and 0.4% phytagel (pH 6.3)] under continuous light conditions at 22 °C. *arr1* (*arr1-3*), *arr2* (*arr2-4*), *arr10* (*arr10-5*), *arr12* (*arr12-1*), *arr1/12* (*arr1-3 arr12-1*), *ahk3/4* (*ahk3-1 ahk4-1*), *ccs52a1* (*ccs52a1-1*), *shy2* (*shy2-31*), *axr2* (*axr2-1*), *rsl4* (*rsl4-1*), and the transgenic lines *pARR1:ARR1-GUS*, *pARR12:ARR12-GUS*, and *pRSL4:GUS* were previously described (Nagpal *et al.*, 2000; Dello Ioio *et al.*, 2008; Yi *et al.*, 2010; Takahashi *et al.*, 2013; Takatsuka *et al.*, 2018). Homozygous *arr1/12 rsl4* triple mutants were identified through PCR using the primers listed in Supplementary Table S1. The chemicals used in this study are *trans*-zeatin (*t*-zeatin; Nacalai Tesque, Kyoto, Japan) and PEO-IAA [2-(1H-indol-3-yl)-4-oxo-4-phenyl-butyric acid; MedChemExpress, NJ, USA).

Plasmid construction

To create *pARR1:ARR1-GFP*, the genomic fragment of *ARR1* from 2000 bp upstream of the start codon to 1 bp before the stop codon was amplified using PCR. The primers used in this process are listed in Supplementary Table S1. The resultant fragment was cloned into the GATEWAY

entry vector pDONR221 (Invitrogen, MA, USA). Next, a recombination reaction was conducted between the entry clone and the GATEWAY destination vector pGWB604 (Nakamura *et al.*, 2010) using LR clonase (Invitrogen) to generate the green fluorescent protein (*GFP*) fusion gene.

To create *pEXP7:ARR1-GFP*, the coding region of *ARR1*, from the start codon to 1 bp before the stop codon, was amplified and cloned into the entry vector pDONR221 (Invitrogen). The primers used in this process are listed in Supplementary Table S1. The resultant entry clone reacted with the entry clone carrying the promoter region of *EXPANSIN A7* (*EXP7*) from 1413 bp upstream of the start codon to 1 bp before the start codon (Shibata *et al.*, 2018) and the destination vector R4pGWB604 (Nakamura *et al.*, 2010) using LR clonase. A fusion gene comprising the *EXP7* promoter, the *ARR1* coding region, and the *GFP* gene was thus generated.

To generate *pRSL4:GUS*, the promoter region of *RSL4* from 3320 bp upstream of the start codon to 1 bp before the start codon was amplified, according to Yi *et al.* (2010), and cloned into the entry vector pDONR221. The primers used in this process are listed in Supplementary Table S1. Next, a recombination reaction was conducted between the entry clone and the destination vector pGWB3 (Nakagawa *et al.*, 2007) using LR clonase to generate a fusion comprising the *RSL4* promoter and the *GUS* (β-glucuronidase) gene.

To obtain *pRSL4(mEBS):GUS*, the entry clone for *pRSL4:GUS* was linearized by PCR using primers designed for site-directed mutagenesis, according to Feng *et al.* (2017). The primers used in this process are listed in Supplementary Table S1. Next, the PCR amplicon carrying the mutations in the EIN3-binding site (EBS) was fused using an In-Fusion HD Cloning Kit (Takara, Shiga, Japan). After DNA sequencing, a recombination reaction was conducted between the resultant entry clone and pGWB3, as described above.

Microscopy

The roots were mounted with distilled water and observed using a stereomicroscope to observe the root hairs (SZX16, Olympus, Tokyo, Japan). The *pARR1:ARR1-GFP* plants were mounted with water and observed under a fluorescence microscope (BX51, Olympus). The *pEXP7:ARR1-GFP* plants were stained with 10 μg ml^{-1} propidium iodide and observed under a confocal laser scanning microscope (A1, Nikon, Tokyo, Japan).

GUS staining

The roots were fixed in 90% (v/v) acetone for 15 min on ice, then were washed with a GUS buffer [100 mM Na_2HPO_4 (pH 7.0), 5 mM $K_3Fe(CN)_6$, 5 mM $K_4Fe(CN)_6$], and immersed in the same buffer containing 0.5 mg ml^{-1} X-gluc (5-bromo-4-chloro-3-indolyl-β-D-glucuronide). The samples were degassed for 15 min and incubated at 37 °C.

Measurement of root hair length and hair growth rate

The root hairs at the region >3 mm away from the root tips were recorded as images and used for root hair measurement. Root hair length was measured using ImageJ (NIH), as described by Yi *et al.* (2010). More than 15 root hairs were randomly selected from 10 individual plants and subjected to measurement. As described previously, the root hair growth rate was measured (Shibata *et al.*, 2018). Briefly, the hair growth of 5-day-old seedlings harboring *pARR1:ARR1-GFP* was recorded every hour using SZX16 (Olympus), and the root hair length was quantified using ImageJ.

Measurement of leaf blade area

The first and second leaves were excised from seedlings at the base of the leaf petiole, and leaf images were taken under a stereomicroscope. The leaf blade area was measured using ImageJ.

Microarray analysis

The seeds were germinated on MS medium and grown under continuous light at 22 °C. The 5-day-old seedlings of the wild type and *arr1/12* were transferred to media containing 1 μM *t*-zeatin or DMSO and grown for 1 h. Total RNA was extracted using the RNeasy Plant Mini Kit (QIAGEN, Venlo, the Netherlands). Microarray analysis was conducted using the Agilent Arabidopsis microarray platform, as previously described (Nguyen *et al.*, 2016). Cyanine-3-labeled cDNA, obtained from total RNA, was hybridized to Agilent-034592 Arabidopsis Custom Microarray. The slide scanning was conducted using an Agilent DNA Microarray Scanner (G2539A ver. C).

Quantitative RT–PCR

Total RNA was extracted using the Plant Total RNA Mini Kit (FAVORGEN, Ping-Tung, Taiwan). According to the manufacturer's instructions, the first-strand cDNA was prepared from the total RNA using ReverTra Ace (Toyobo, Osaka, Japan). Quantitative reverse transcription–PCR (qRT–PCR) was conducted using the THUNDERBIRD SYBR qPCR Mix (Toyobo). The primer sequences used for *RSL4* and *EUKARYOTIC TRANSLATION INITATION FACTOR* (*eIF*) quantification are listed in Supplementary Table S1. PCRs was conducted using the StepOnePlus Real-Time PCR System (Applied Biosystems) under the following conditions: 95 °C for 60 s; 60 cycles at 95 °C for 10 s, at 55°C for 30 s, and at 72°C for 30 s; 95 °C for 15 s; 55 °C for 60 s; and 95 °C for 15 s.

ChIP-qPCR

ChIP-qPCR analysis was performed using 7-day-old wild-type (Col-0) seedlings and *pARR1:ARR1-GFP* as described previously (Favero *et al.*, 2020), with minor differences. About 2 g of plant roots were harvested and frozen using liquid nitrogen. The frozen samples were ground using a Multi-beads shocker (Yasui Kikai, Osaka, Japan) at 2400 Hz for three cycles of 10 s each and subsequently soaked in a fixation buffer for 10 min. For genomic DNA fragmentation, Picoruptor 2 (Diagenode, Liège, Belgium) was used for 10 cycles, 30 s on/30 s off. The sonicated DNA fragments were immunoprecipitated using Dynabeads Protein G (Thermo Fisher Scientific, MA, USA) and an anti-GFP antibody (Abcam, Cambridge, UK).

Quantitative real-time PCR was performed using the THUNDERBIRD SYBR qPCR Mix (Toyobo) with the primers indicated in Supplementary Table S1. For each of the two biologically independent chromatin preps, ChIP was performed in triplicate. Data were normalized against input DNA. The *TA3* retrotransposon locus was also used as an additional negative control (Yamaguchi *et al.*, 2014).

AlphaScreen assay

The interaction between *in vitro* translated ARR1 protein and dsDNA was performed as previously described (Tokizawa *et al.*, 2015). The FLAG-tagged ARR1 proteins were synthesized using an *in vitro* transcription/translation system (NUProtein; Tokushima, Japan). Both biotinylated and non-biotinylated DNA oligos used in the assays are listed in Supplementary Table S1. The acceptor and donor beads for the AlphaScreen detection were coated with the anti-FLAG antibody and streptavidin, respectively. The beads were labeled with the FLAG-tagged ARR1 protein or the biotinylated dsDNA-oligo using the AlphaScreen FLAG (M2) Detection Kit (PerkinElmer, MA, USA), following the manufacturer's protocols. The AlphaScreen signals, which correspond to the chemiluminescence intensity caused by the binding between the donor and acceptor beads, were determined with the EnSight Multimode plate reader (PerkinElmer).

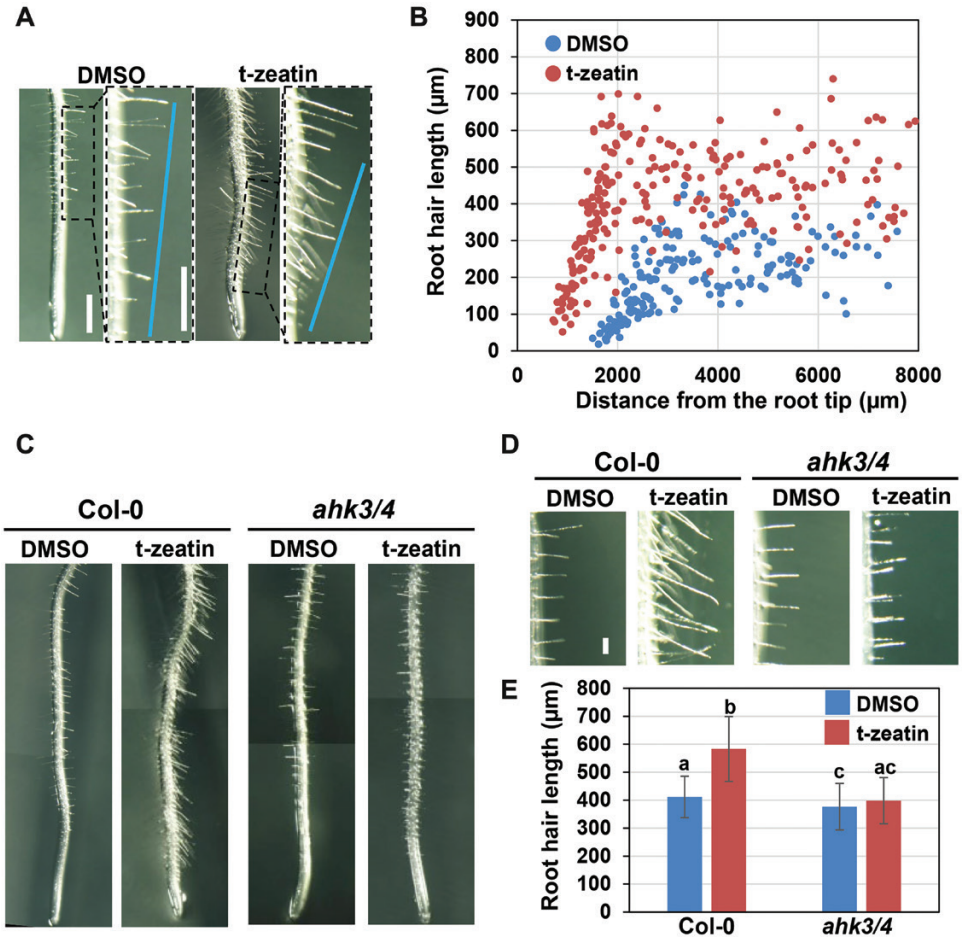

Fig. 1. CK promotes root hair elongation through AHK3 and AHK4. (A) Representative images of wild-type roots grown in the presence or absence of *t*-zeatin. Magnified images of the root hair-developing zone are shown on the right. Five-day-old seedlings were transferred to MS medium containing 0 nM (DMSO) or 50 nM *t*-zeatin, and further grown for 3 d. The scale bars represent 500 μm. (B) A scatter plot of the root hair length and distance from the root tip in plants treated with or without *t*-zeatin, as shown in (A). H cells randomly selected from six seedlings were subjected to quantification. (C) Roots of wild-type (Col-0) and *ahk3/4* seedlings. Five-day-old seedlings were transferred to MS medium containing DMSO (mock) or 50 nM *t*-zeatin and further grown for 3 d. The scale bar represents 500 μm. (D) Magnified images of root hairs shown in (C). The scale bar represents 100 μm. (E) Length of mature root hairs in the wild type and *ahk3/4*. Data are presented as mean ±SD (n>150). Bars with different letters significantly differ from each other. Significant differences were determined using Tukey's test (P<0.05).

Results

ARR1 and ARR12 regulate CK-dependent root hair elongation

To first confirm the promotive role of CK in root hair elongation, Arabidopsis roots were grown in the presence of 50 nM *t*-zeatin for 3 d. The result indicated that longer root hairs were formed from *t*-zeatin-treated seedlings, as previously reported (Fig. 1A; see also Fig. 1E) (Su and Howell, 1992; An *et al.*, 2012; Zhang *et al.*, 2016). To understand how CK affects root hair length, we plotted the hair length against the distance from the root tip according to the method described previously (Kato *et al.*, 2019). The data indicated that, in *t*-zeatin-treated samples, root hairs became visible in the region proximal to the root tip and reached the maximum length earlier than in mock-treated samples (Fig. 1B). This result indicates that CK facilitates root hair elongation through accelerating hair growth, rather than by prolonging the period of hair elongation.

During root hair development, cell fate specification and subsequent hair initiation are known to affect the final hair length (Zhang *et al.*, 2016); therefore, whether CK alters the H/N cell fate was examined by counting hair-producing N cells in the N cell lineage. According to the result, the *t*-zeatin treatment, even at a higher concentration of 250 nM, did not promote ectopic root hair formation in the N cell lineage (Supplementary Fig. S1A, B). We also counted the H cells lacking root hairs in the differentiated region and discovered that the *t*-zeatin treatment did not significantly decrease the ratio of the cells without root hairs in the H cell lineage (Supplementary Fig. S1C). These results suggest that CK is not associated with cell fate specification.

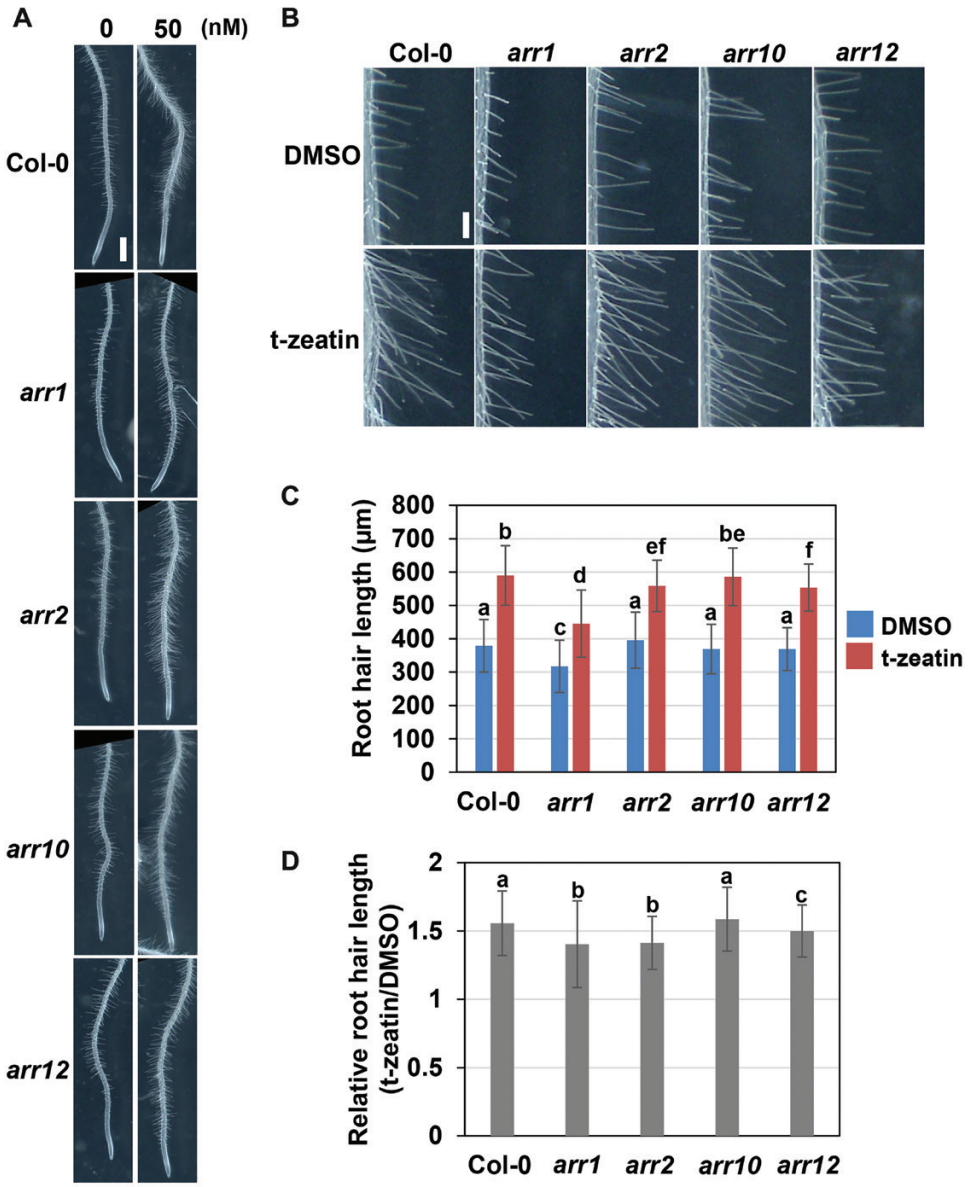

Fig. 2. ARR1, ARR2, and ARR12 are involved in CK-induced root hair elongation. (A) Roots of the wild type (Col-0), *arr1*, *arr2*, *arr10*, and *arr12*. Five-day-old seedlings were transferred to MS medium containing 0 nM (DMSO) or 50 nM *t*-zeatin and further grown for 3 d. The scale bar represents 500 μm. (B) Magnified images of root hairs shown in (A). The scale bar represents 100 μm. (C) Length of mature root hairs in the wild type, *arr1*, *arr2*, *arr10*, and *arr12*. Data are presented as mean ±SD (n>150). Bars with different letters significantly differ from each other. Significant differences were determined using Tukey's test (P<0.05). (D) Relative root hair length of *t*-zeatin-treated roots is indicated as relative values, where the mean root hair length of the non-treated roots of each genotype is taken as 1. Bars with different letters significantly differ from each other. Significant differences were determined using Tukey's test (P<0.05).

We then asked whether CK regulates root hair elongation through the phosphorelay pathway. First, we observed the phenotype of the double knockout mutant defective in the CK receptor genes *AHK3* and *AHK4*. As shown in Fig. 1C–E, root hair length was slightly but significantly shorter in *ahk3/4* than in the wild type. Treatment with 50 nM *t*-zeatin increased the root hair length in the wild type but not in *ahk3/4* (Fig. 1C–E). This result indicates that *AHK3* and *AHK4* are involved in the CK-triggered enhancement of root hair elongation.

Among 24 *ARR* genes, 11 genes encode B-type ARRs: *ARR1*, *ARR2*, *ARR10*, *ARR11*, *ARR12*, *ARR13*, *ARR14*, *ARR18*, *ARR19*, *ARR20*, and *ARR21* (Hill *et al.*, 2013). Normalized microarray data on the Arabidopsis electronic fluorescent pictograph (eFP) browser (Brady *et al.*, 2007) showed that *COBRA-LIKE 9* (*COBL9*) and *RSL4*, whose mRNA levels increase during root hair growth (Yi *et al.*, 2010; Huang *et al.*, 2017; Jean-Baptiste *et al.*, 2019), are expressed from root zones #6 to #10, while *ARR1*, *ARR2*, *ARR10*, and *ARR12* are transcribed from zones #6 to

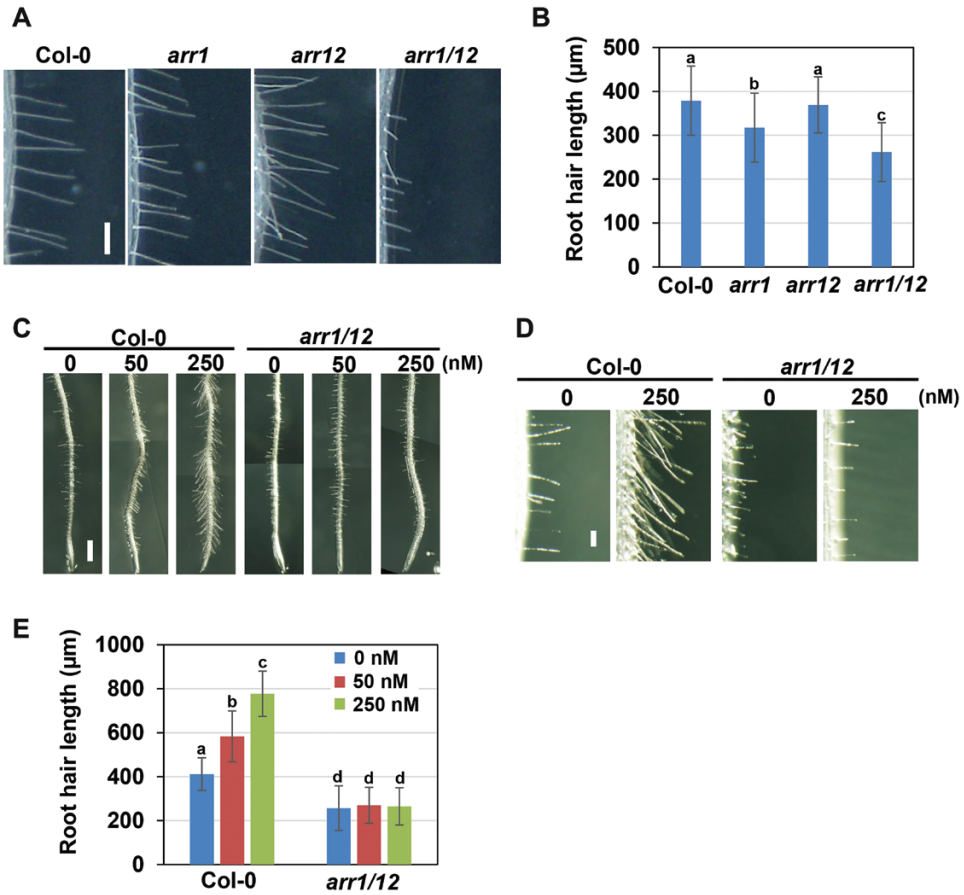

Fig. 3. CK-induced root hair elongation is suppressed in *arr1/12*. (A) Root hairs of 8-day-old seedlings of the wild type (Col-0), *arr1*, *arr12*, and *arr1/12*. The scale bar represents 100 μm. (B) Length of mature root hairs in the wild type, *arr1*, *arr12*, and *arr1/12*. Data are presented as mean ±SD (n>150). Bars with different letters significantly differ from each other. Significant differences were determined using Tukey's test (P<0.05). (C) Roots of the wild type and *arr1/12*. Five-day-old seedlings were transferred to MS medium containing 0 nM (DMSO), 50 nM, or 250 nM *t*-zeatin and further grown for 3 d. The scale bar represents 500 μm. (D) Magnified images of root hairs shown in (C). The scale bar represents 100 μm. (E) Length of mature root hairs in the wild type and *arr1/12*. Data are presented as mean ±SD (n>150). Bars with different letters significantly differ from each other. Significant differences were determined using Tukey's test (P<0.05).

#10 and in more apical and basal regions (Supplementary Fig. S2). Other B-type *ARR* genes were barely expressed in the roots, whereas *ARR20* was excluded in the microarrays. Since Mason *et al.* (2004) reported that *ARR20* transcripts were not detected in roots using RT–PCR, we decided to focus on *ARR1*, *ARR2*, *ARR10*, and *ARR12* for further analysis.

To identify the B-type ARR(s) involved in root hair elongation, we measured the root hair length of knockout mutants. In the *arr1* mutant, mature root hairs were significantly shorter than in the wild type, whereas the hair length of *arr2*, *arr10*, and *arr12* was comparable with that of the wild type (Fig. 2A–C); this suggests that ARR1 plays a major role in root hair elongation. However, when 50 nM *t*-zeatin was applied, enhanced hair growth was not fully suppressed in *arr1*, and such partial suppression was also observed in *arr2* and *arr12* (Fig. 2C, D). This indicates that B-type ARRs other than ARR1 also participate in CK-dependent root hair elongation. Indeed, the root hairs of the *arr1 arr12* double mutant (*arr1/12*) were shorter than those of either the *arr1* or *arr12* single mutants (Fig. 3A, B) and were insensitive to exogenously applied *t*-zeatin (Fig. 3C–E). Since the effect of 250 nM *t*-zeatin was more significant than that of 50 nM *t*-zeatin in the wild type and fully suppressed in *arr1/12* (Fig. 3E), we then used 250 nM *t*-zeatin for CK treatment and focused on ARR1/12 as B-type ARRs controlling root hair elongation. As shown in Supplementary Fig. S3, a 3 d treatment with 250 nM *t*-zeatin did not significantly affect shoot growth in the wild type and the mutants used in this study, except in *ein3 eil1* (see the section below). This result indicates that the root hair phenotype observed in these experiments was not a consequence of altered shoot development.

ARR1 and ARR12 proteins accumulate in growing root hairs to promote root hair elongation

According to previous studies, ARR1 and ARR12 proteins accumulate in the area encompassing the transition zone (TZ)

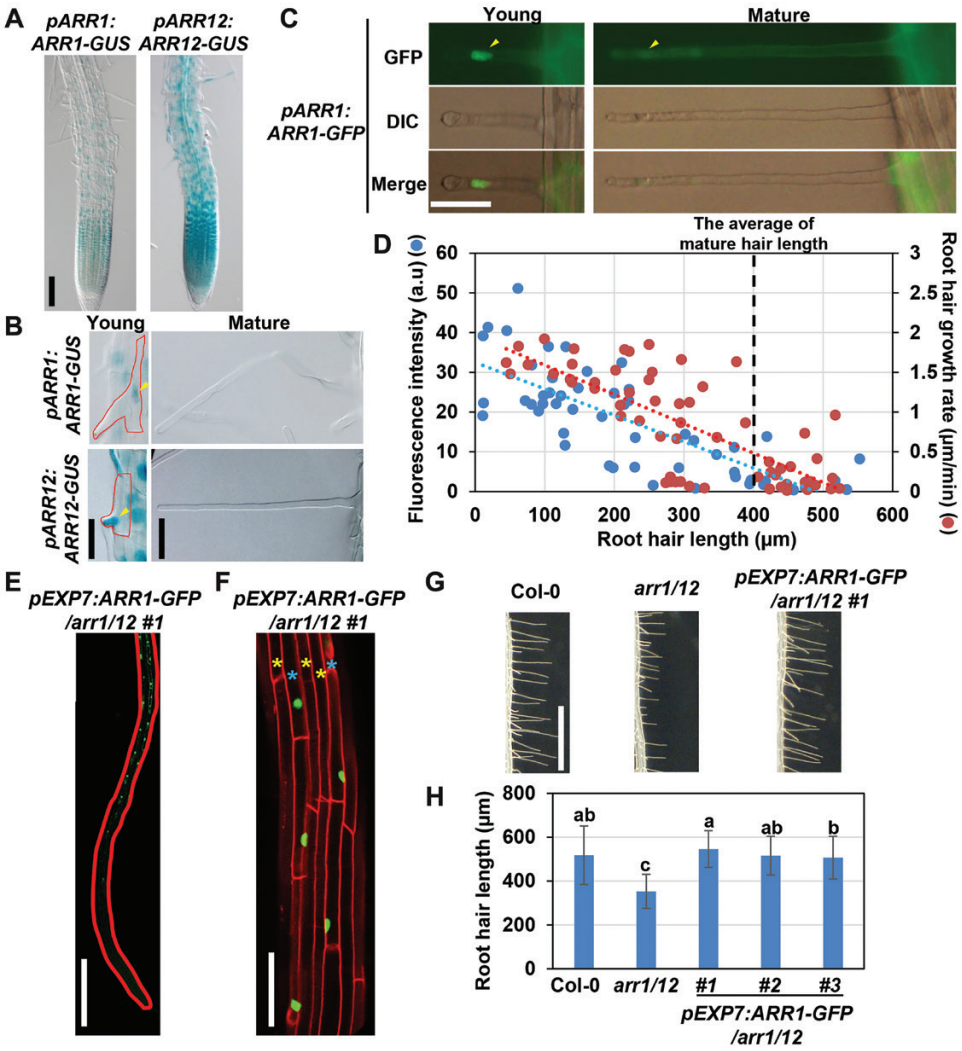

Fig. 4. ARR1 and ARR12 proteins accumulate during root hair elongation. (A and B) Roots and root hairs of GUS-stained 5-day-old transgenic plants harboring *pARR1:ARR1-GUS* or *pARR12:ARR12-GUS*. Red lines and yellow arrowheads indicate cell outlines and nuclei, respectively. The scale bars represent 100 μm. (C) Root hairs in 5-day-old roots harboring *pARR1:ARR1-GFP*. Yellow arrowheads indicate nuclei. The scale bar represents 50 μm. (D) Scatter diagram plotting GFP fluorescence intensity (blue dots) and root hair growth rate (red dots) against root hair length. Blue and red dotted lines indicate approximate straight lines for fluorescence intensity and root hair growth rate, respectively. (E) Five-day-old root of the *arr1/12* double mutant carrying *pEXP7:ARR1-GFP*. A red line traced the outline of the root. The scale bar represents 500 μm. (F) Magnified image of (E). The outlines of cells were visualized by propidium iodide. Blue and yellow asterisks represent the H and N cell lineages, respectively. The scale bar represents 100 μm. (G) Root hairs of 5-day-old seedlings of the wild type (Col-0), *arr1/12*, and *arr1/12* carrying *pEXP7:ARR1-GFP*. The scale bar represents 1 mm. (H) Length of mature root hairs in the wild type, *arr1/12*, and three independent lines of *arr1/12* carrying *pEXP7:ARR1-GFP*. Data are presented as mean ±SD (n>150). Bars with different letters display significant differences determined using Tukey's test (P<0.05).

(Dello Ioio et al., 2007, 2008; Xie *et al.*, 2018; Takatsuka and Umeda, 2019), while their expression patterns during root hair development remain unknown. Therefore, the protein accumulation of ARR1/12 was observed using translational reporter genes fused with *GUS*, driven by their own promoters. In both reporter lines, GUS signal was observed in both H and N cells (Fig. 4A). Closer observation of the H cell lineage revealed that the GUS signal was detected in the nuclei of young root hairs, but not in fully elongated hairs that resided >5 mm away from the root tip (Fig. 4B). The GFP reporter line for *ARR1* (*pARR1:ARR1-GFP*) displayed a similar expression pattern to that of the *GUS* reporter line; the GFP intensity was higher in rapidly elongating short hairs than in the slowly growing longer ones, and mature hairs that stopped elongation barely showed GFP fluorescence (Fig. 4C, D). These results suggest that ARR1/12 proteins accumulate in growing root hairs but gradually disappear as hair elongation proceeds.

We conducted a complementation test to examine whether the ARR1 protein accumulation in H cells is indeed associated with CK-dependent root hair elongation. When ARR1–GFP was expressed under the *EXPANSIN A7* (*EXP7*) promoter, which is active in the H cell lineage (Fig. 4E, F), the short hair

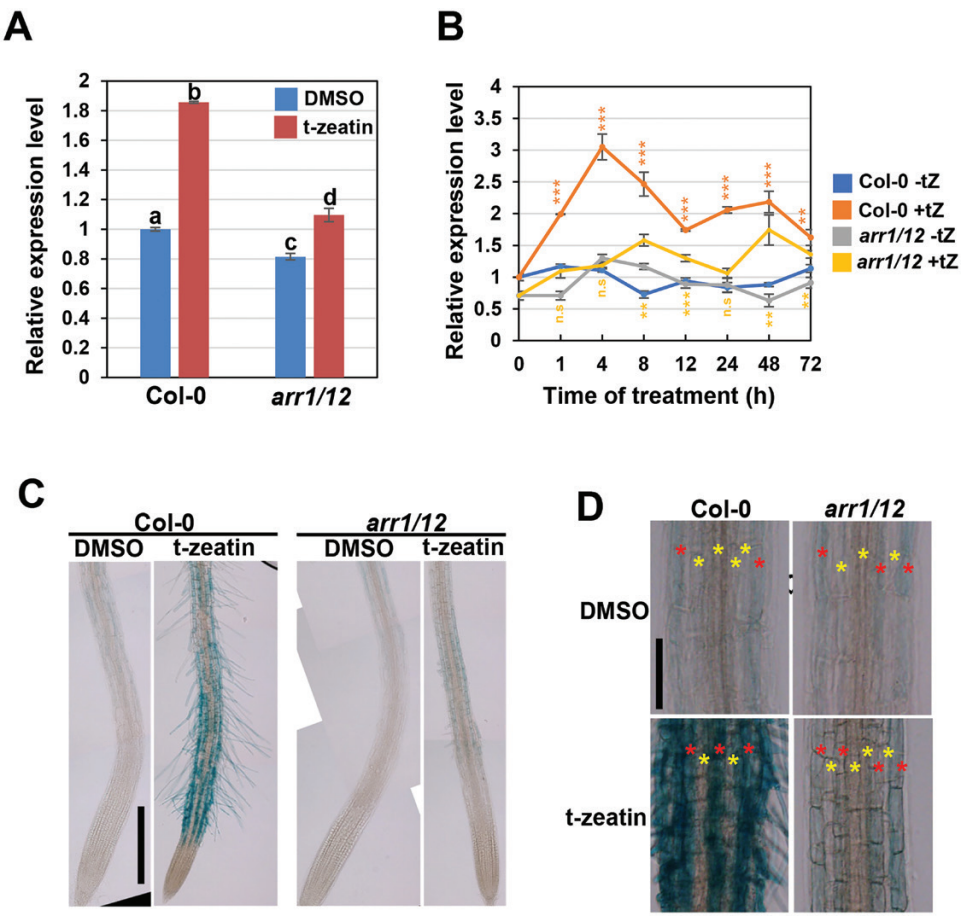

Fig. 5. CK induces *RSL4* expression via ARR1 and ARR12. (A) Transcript levels of *RSL4* determined using qRT–PCR. Five-day-old roots of the wild type (Col-0) and *arr1/12* were transferred to MS medium containing 250 nM *t*-zeatin and further grown for 3 d. Total RNA was extracted from root tips. Data are presented as mean ±SD (n=3). mRNA levels are indicated as relative values, with that for non-treated wild type (DMSO) set to 1. Bars with different letters significantly differ from each other. Significant differences were determined using Tukey's test (P<0.05). (B) Time-course monitoring of *RSL4* transcripts. Five-day-old seedlings of the wild type and *arr1/12* double mutants were transferred to MS plates with or without 250 μM *t*-zeatin and grown for 0, 1, 4, 8, 12, 24, 48, and 72 h. mRNA levels obtained by qRT–PCR are indicated as relative values, with the value for the non-treated wild type set to 1. (C) GUS staining of roots of the wild type and *arr1/12* harboring *pRSL4:GUS* treated with or without *t*-zeatin under the same conditions as in (A). The scale bar represents 500 μm. (D) Magnified images of root hairs shown in (C). Red and yellow asterisks represent H and N cell lineages, respectively.

phenotype of the *arr1/12* double mutants was fully suppressed in three independent lines (Fig. 4G, H). This result suggests that ARR1 accumulation in H cells promotes root hair elongation.

CCS52A1 and SHY2 are not required for CK-dependent root hair elongation

CK inhibits cell division and promotes endoreplication in the TZ of Arabidopsis roots (Dello Ioio *et al.*, 2008; Takahashi *et al.*, 2013). ARR2 is known to induce *CCS52A1*, which encodes the substrate-specific activator of the APC/C, thereby enhancing the degradation of mitotic cyclins and triggering endoreplication (Takahashi *et al.*, 2013). Cell expansion is often associated with endoreplication (Larson-Rabin *et al.*, 2009), and ARR2 participates in CK-dependent root hair elongation (Fig. 2); therefore, we first examined the involvement of CCS52A1. In the absence of *t*-zeatin, mature root hair length was slightly but significantly shorter in the *ccs52a1* knockout mutant than in the wild type, suggesting the role of CCS52A1 in root hair elongation (Supplementary Fig. S4A, B). However, *ccs52a1* responded to *t*-zeatin to the same extent as the wild type, implying that CCS52A1 is not involved in the CK-mediated regulation of root hair growth (Supplementary Fig. S4A–C). We then focused on *SHY2*, which is up-regulated by ARR1/12 around the TZ and inhibits auxin signaling by repressing *PIN* genes, leading to cell cycle retardation (Dello Ioio *et al.*, 2008; Takahashi *et al.*, 2021). However, the *shy2* knockout mutant displayed no significant difference in root hair length compared with the wild type, irrespective of exogenous *t*-zeatin treatment (Supplementary Fig. S4D–F). These results suggest that CK signaling controls root hair growth through downstream factor(s) other than CCS52A1 or SHY2.

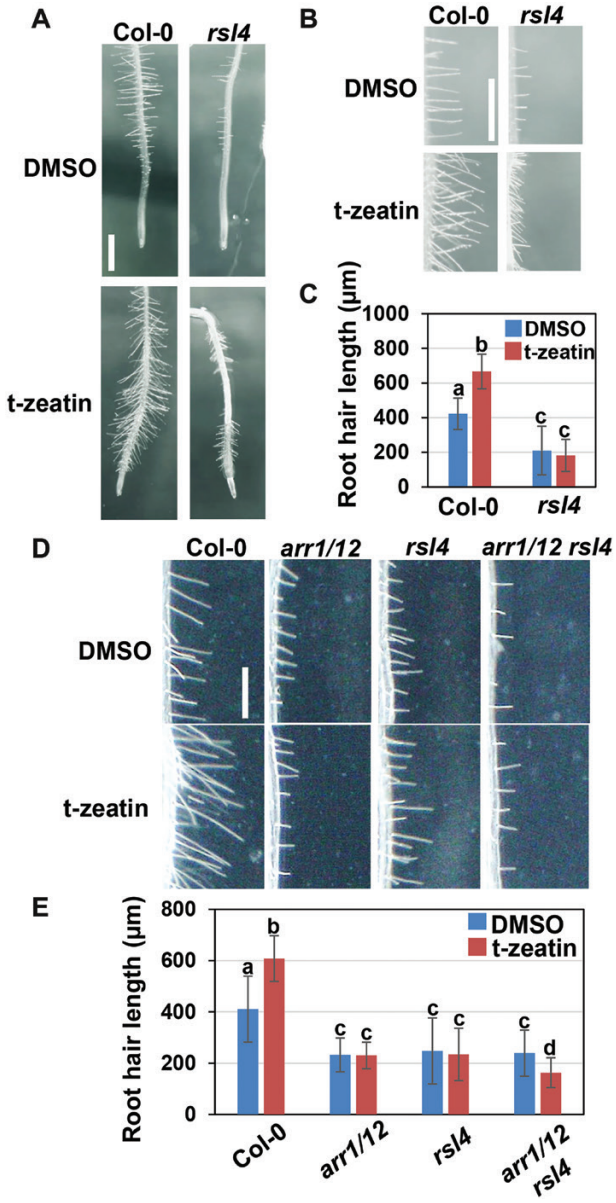

Fig. 6. CK-induced root hair elongation requires *RSL4*. (A) Roots of the wild type (Col-0) and *rsl4*. Five-day-old seedlings were transferred to MS medium containing 0 nM (DMSO) or 250 nM *t*-zeatin and further grown for 3 d. The scale bar represents 500 μm. (B) Magnified images of root hairs shown in (A). The scale bar represents 500 μm. (C) Length of mature root hairs in the wild type and *rsl4*. Data are presented as mean ±SD (n>150). Bars with different letters significantly differ from each other. Significant differences were determined using Tukey's test (P<0.05). (D) Magnified images of root hairs of the wild type, *arr1/12*, *rsl4*, and *arr1/12 rsl4*. Five-day-old seedlings were transferred to MS medium containing DMSO (mock) or 250 nM *t*-zeatin and further grown for 3 d. The scale bar represents 500 μm. (E) Length of mature root hairs in the wild type, *arr1/12*, *rsl4*, and *arr1/12 rsl4*. Data are presented as mean ±SD (n>150). Bars with different letters significantly differ from each other. Significant differences were determined using Tukey's test (P<0.05).

CK promotes root hair elongation via RSL4

To identify the downstream gene(s) of ARR1/12 that regulate CK-dependent root hair elongation, microarray analysis was conducted using RNA extracted from the root tips of the wild type and *arr1/12*, which were treated with 1 μM *t*-zeatin for 1 h. We selected 321 genes that satisfy the following three conditions: (i) *t*-zeatin treatment should increase mRNA levels by >50% in the wild type; (ii) mRNA levels should be <90% in *arr1/12* compared with those in the wild type in the absence of *t*-zeatin; and (iii) the rate of increase in mRNA levels after *t*-zeatin treatment should be <25% in *arr1/12* compared with those in the wild type. The list includes direct target genes of ARR1, such as *ARR15* and *SHY2* (Taniguchi *et al.*, 2007), and *RSL4*, the central regulator for root hair elongation (Supplementary Table S2; Supplementary Fig. S5).

When the qRT–PCR analysis was conducted using RNA extracted from roots that were treated with 250 nM *t*-zeatin for 3 d, the same trend was observed for *RSL4* mRNA levels (Fig. 5A). The slight increase observed in *arr1/12* upon a 250 nM *t*-zeatin treatment is likely to be due to the negative feedback regulation mediated by A-type ARRs that is less effective than that caused by 1 μM *t*-zeatin application. Indeed, our time-course experiment performed on wild-type plants grown in the presence of 250 nM *t*-zeatin indicated that the *RSL4* mRNA level increased at 1 h and reached the maximum at 4 h, while even at 72 h, it was significantly higher than that of the mock samples (Fig. 5B). The gene-trap line representing the *RSL4* expression (Yi *et al.*, 2010) also displayed an apparent response to *t*-zeatin in the wild type but was not significant in *arr1/12* (Fig. 5C). It is noteworthy that this CK response was observed only in the H cell lineage (Fig. 5D).

To reveal the functional role of *RSL4* in CK-dependent root hair elongation, the *rsl4-1* knockout mutant was treated with *t*-zeatin. This mutant formed short root hairs, as previously reported (Yi *et al.*, 2010), and exhibited no enhancement in root hair growth after *t*-zeatin treatment (Fig. 6A–C). Moreover, the *arr1/12 rsl4* triple mutant exhibited neither an additive nor a synergistic phenotype compared with *arr1/12* or *rsl4* (Fig. 6D, E), indicating that *ARR1/12* and *RSL4* function in the same pathway. These results suggest that CK induces *RSL4* through ARR1/12, thereby promoting root hair elongation.

CK facilitates root hair elongation independently of ethylene or auxin signaling

Since CK is known to affect ethylene signaling in some cases (Cary *et al.*, 1995; Růžička *et al.*, 2009), we tested the possibility that the ARR1/12-dependent *RSL4* induction is controlled through ethylene signaling. A previous study demonstrated that ethylene activates the key transcription factors EIN3 and EIL1 that directly induce *RSL4* to promote root hair growth (Feng *et al.*, 2017). Therefore, we first examined the transcriptional response of *RSL4* to CK in

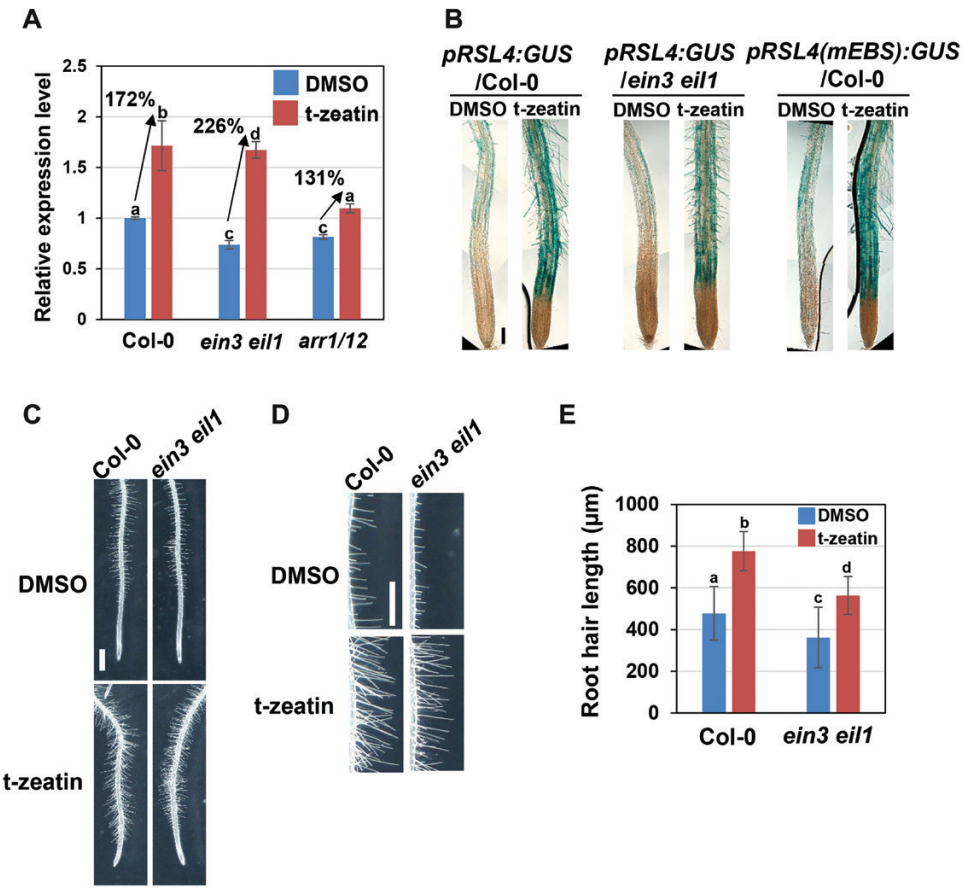

Fig. 7. Ethylene signaling is not involved in CK-induced *RSL4* expression and root hair elongation. (A) Transcript levels of *RSL4* determined using qRT–PCR. Five-day-old roots of the wild type (Col-0), *ein3 eil1*, and *arr1/12* were transferred to MS medium containing DMSO (mock) or 250 nM *t*-zeatin, and further grown for 3 d. Total RNA was extracted from root tips. Data are presented as mean ±SD (n=3). mRNA levels are indicated as relative values, with that for the non-treated wild type (DMSO) set to 1. Bars with different letters significantly differ from each other. Significant differences were determined using Tukey's test (P<0.05). (B) GUS staining of roots of the wild type and *ein3 eil1* harboring *pRSL4:GUS*, and the wild-type carrying *pRSL4(mEBS):GUS*. Roots were treated with or without (DMSO) 250 nM *t*-zeatin for 3 d. The scale bar represents 100 μm. (C) Roots of the wild type and *ein3 eil1*. Five-day-old seedlings were transferred to MS medium containing DMSO (mock) or 250 nM *t*-zeatin, and further grown for 3 d. The scale bar represents 500 μm. (D) Magnified images of (C). The scale bar represents 1 mm. (E) Length of mature root hairs in the wild type and *ein3 eil1*. Data are presented as mean ±SD (n>150). Bars with different letters significantly differ from each other. Significant differences were determined using Tukey's test (P<0.05).

the *ein3 eil1* double knockout mutants, in which ethylene-dependent *RSL4* induction is completely suppressed (Feng *et al.*, 2017). In the absence of exogenous *t*-zeatin, the transcript level of *RSL4* was lower in *ein3 eil1* compared with the wild type. In contrast, a 250 nM *t*-zeatin treatment led to an increase of *RSL4* transcripts in the mutant to a higher level than in the wild type (Fig. 7A). To analyze the *RSL4* expression at the tissue level, we generated a reporter gene in which the 3.3 kb genomic fragment upstream of the transcription start site (TSS), which is sufficient to represent the native expression pattern (Yi *et al.*, 2010), was fused to the *GUS* gene. We then introduced it into wild-type and *ein3 eil1* plants. As shown in Fig. 7B, *t*-zeatin treatment greatly elevated the *GUS* expression in *ein3 eil1*, as in the wild type. Moreover, the mutations at the EBS on the *RSL4* promoter, which are known to compromise the EIN3-dependent induction of *RSL4* (Feng *et al.*, 2017), did not affect the response to *t*-zeatin (Fig. 7B). These results indicate that the CK-dependent *RSL4* induction does not require the EIN3/EIL1-mediated ethylene signaling.

As previously reported, the *ein3 eil1* double mutant formed shorter root hairs than the wild type (Feng *et al.*, 2017) (Fig. 7C–E). However, *t*-zeatin application significantly increased the root hair length in *ein3 eil1* (Fig. 7C–E). In *ein3 eil1*, the leaf size was reduced by *t*-zeatin treatment but was still comparable with that of *t*-zeatin-treated wild-type leaves (Supplementary Fig. S3). This result suggests that the CK-induced root hair elongation observed in *ein3 eil1* is not a consequence of altered shoot growth. Overall, these results indicate that ethylene signaling is dispensable for CK-induced root hair elongation.

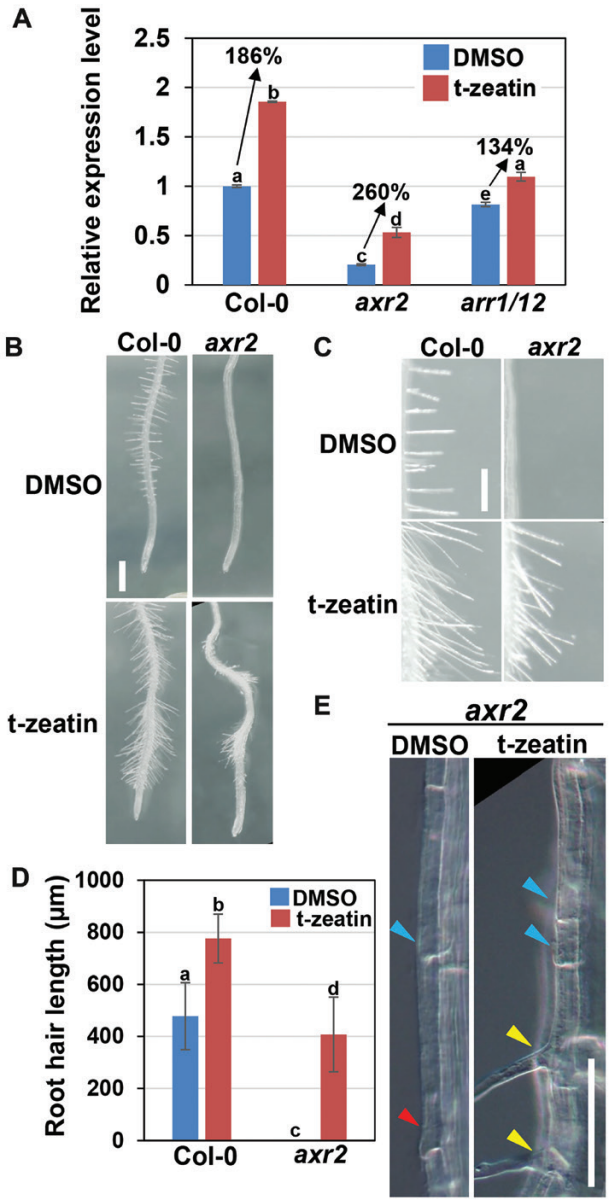

Fig. 8. CK induces *RSL4* expression and enhances root hair elongation in *axr2*. (A) Transcript levels of *RSL4* determined using qRT–PCR. Five-day-old roots of the wild type (Col-0), *axr2*, and *arr1/12* were transferred to MS medium containing DMSO (mock) or 250 nM t-zeatin and grown for 3 d. Total RNA was extracted from root tips. Data are presented as mean ±SD (n=3). mRNA levels are indicated as relative values, with the value for the non-treated wild type set to 1. Bars with different letters display significant differences determined using Tukey's test (P<0.05). (B) Roots of the wild type and *axr2*. Five-day-old seedlings were transferred to MS medium containing DMSO (mock) or 250 nM *t*-zeatin and grown for 3 d. The scale bar represents 500 μm. (C) Magnified images of (B). The scale bar represents 500 μm. (D) Length of mature root hairs in the wild type and *axr2*. Data are presented as mean ±SD (n>150). Bars with different letters display significant differences determined using Tukey's test (P<0.05). (E) Hair cells of the wild type and *axr2* treated with or without 250 nM *t*-zeatin for 3 d. Blue, red, and yellow arrowheads represent H cells without a bulge, with a bulge, and with a protruding root hair, respectively. The scale bar represents 100 μm.

Previous studies have demonstrated that auxin as well as ethylene positively regulates *RSL4* expression and promotes root hair elongation (López-Bucio *et al.*, 2003; Guimil and Dunand, 2007; Ishida *et al.*, 2008; Yi *et al.*, 2010; Feng *et al.*, 2017). Therefore, to test whether auxin signaling is associated with CK-induced *RSL4* expression, we used *auxin resistant 2-1* (*axr2-1*; hereafter called *axr2*), a dominant mutant of *AXR2/IAA7* that encodes an Aux/IAA transcriptional repressor (Timpte *et al.*, 1994). In this mutant, root hair growth is arrested before or soon after bulge formation in H cells, leading to a complete loss of protruding root hairs, indicating that the *axr2-1* mutation reduces auxin signaling below the level required for the initiation and subsequent elongation of root hairs (Nagpal *et al.*, 2000; Muto *et al.*, 2007). Indeed, the transcript level of *RSL4* was drastically decreased in *axr2* compared with the wild type (Fig. 8A). However, after *t*-zeatin treatment, the *RSL4* mRNA level was elevated in *axr2* more than that observed in the wild type (Fig. 8A). In *axr2*, we still frequently observed mature H cells without hair bulges (Fig. 8B, E), probably due to the defect in root hair initiation as mentioned above. Nevertheless, when observing H cells that had already initiated hair elongation, the *t*-zeatin application partially restored the short hair phenotype of *axr2* (Fig. 8B–D). Similar results were also obtained when wild-type roots were treated with the auxin antagonist PEO-IAA (Nishimura *et al.*, 2009); namely, in the presence of 10 μM PEO-IAA, *RSL4* expression and root hair formation were drastically suppressed, whereas *t*-zeatin treatment significantly increased the *RSL4* mRNA level, enhancing root hair elongation (Supplementary Fig. S6). Note that *t*-zeatin application did not affect shoot growth in *axr2* or PEO-IAA-treated wild type (Supplementary Fig. S3). These results suggest that CK induces *RSL4* and promotes root hair growth independently of auxin signaling.

RSL4 *is a direct target of ARR1*

The above results indicate that ARR1 and ARR12 up-regulate *RSL4* through unknown pathways, with the possibility that they directly induce *RSL4* expression. In the 2 kb promoter region of *RSL4*, we found 15 potential core CK response *cis*-elements, (A/G)GAT(T/C), hereafter referred to as CREs (Ramireddy *et al.*, 2013). Interestingly, one of them, which resides 1425 bp upstream of the TSS, met the conditions of the more stringent ARR1-specific extended element (AEE), AAGAT(T/C)TT (Sakai *et al.*, 2001) (Fig. 9A). Therefore, we examined the binding of ARR1 to this motif by AlphaScreen, which can monitor the interaction between *in vitro* translated proteins and biotin-labeled dsDNA (Tokizawa *et al.*, 2015). The measurement of chemiluminescence produced by ARR1-fused acceptor beads, which bind to dsDNA fused to donor beads, showed that the ARR1 protein physically interacts with the AEEs on the *RSL4* and *ARR6* promoters, the latter of which is known to be directly targeted by ARR1 (Fig. 9B). No significant interaction was detected for

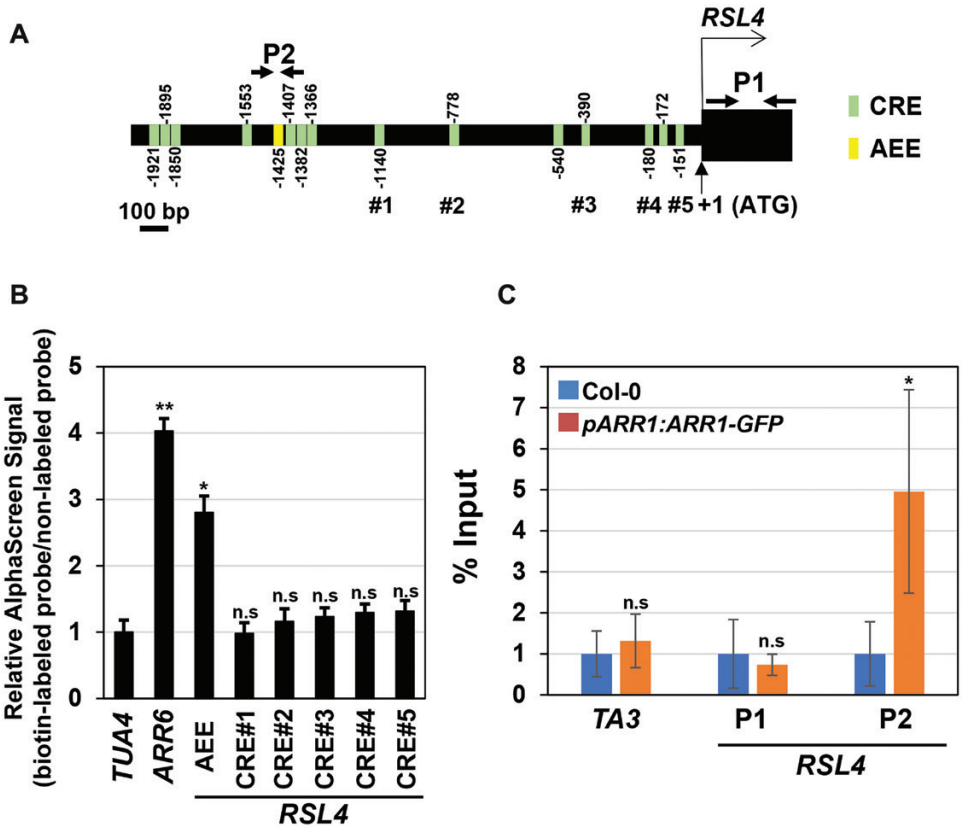

Fig. 9. ARR1 directly binds to the *RSL4* promoter. (A) Schematic representation of the *RSL4* promoter region. The promoter and the gene body are indicated by a black line and a black box, respectively. The cytokinin-response elements (CREs) and the ARR1-specific extended element (AEE) are shown in pink and yellow, respectively. The CREs subjected to AlphaScreen are indicated as #1 to #5. P1 and P2 are the regions amplified by ChIP-qPCR. (B) *In vitro* binding assay of dsDNA and the ARR1 protein using an AlphaScreen system. *In vitro* translated ARR1 proteins labeled with the acceptor beads of the AlphaScreen system were co-incubated with dsDNA probes. Relative AlphaScreen signals were calculated as the ratio of the signals of the biotin-labeled probe to those of the non-biotin-labeled probe. Data are presented as mean ±SD (n=3). Student's t-test was used to determine significant differences from the negative control *TUA4*: *P<0.05; **P<0.01; n.s, not significant. (C) ChIP-qPCR of *RSL4*. ChIP experiments were performed using roots of wild-type (Col-0) seedlings carrying *pARR1:ARR1-GFP*. The average enrichment of qPCR products was normalized against corresponding input DNA. The *TA3* retrotransposon was used as a negative control. Data are presented as mean ±SD (n=3). Student's t-test was used to determine significant differences from the wild type without *pARR1:ARR1-GFP*: *P<0.05; n.s, not significant.

the other five CREs (Fig. 9B). To examine the ARR1 binding *in vivo*, we conducted ChIP-qPCR using the *pARR1:ARR1-GFP* lines. The data indicated that ARR1–GFP proteins bind to the *RSL4* genomic region containing the AEE (P2) but not to the gene body (P1) (Fig. 9C). These results suggest that ARR1/12 directly up-regulate *RSL4*, thereby promoting root hair growth.

Discussion

The promotive effect of exogenously applied CK on root hair elongation has been demonstrated in previous studies (Su and Howell, 1992; An *et al.*, 2012; Zhang *et al.*, 2016). However, thus far, whether, and if so how, the two-component CK signaling pathway is involved in root hair growth has been largely unknown. In this study, we showed that the canonical CK signaling pathway consisting of the receptors AHK3/4 and B-type ARRs ARR1/12 is involved in enhancing root hair elongation (Fig. 10). We then investigated the downstream genes of ARR1/12 and identified *RSL4* as a crucial regulator of CK-dependent root hair growth (Fig. 10). Notably, *RSL4* expression was slightly but significantly elevated in *arr1/12* after *t*-zeatin treatment (Fig. 5A), suggesting that B-type ARR(s) other than ARR1/12 also participate in *RSL4* induction. This idea is supported by our observation that the *arr2* mutant was partially tolerant to 50 nM *t*-zeatin in terms of root hair growth (Fig. 2). Therefore, we speculate that, in hair cells, multiple B-type ARRs fine-tune *RSL4* expression and root hair elongation to respond to changing environments that alter CK levels to various extents. However, it remains obscure how each B-type ARR has been functionally diverged in controlling root hair elongation. Among the knockout mutants of four B-type *ARR* genes, *ARR1*, *ARR2*, *ARR10*, and *ARR12*, only *arr1* displayed an obvious difference from the wild type

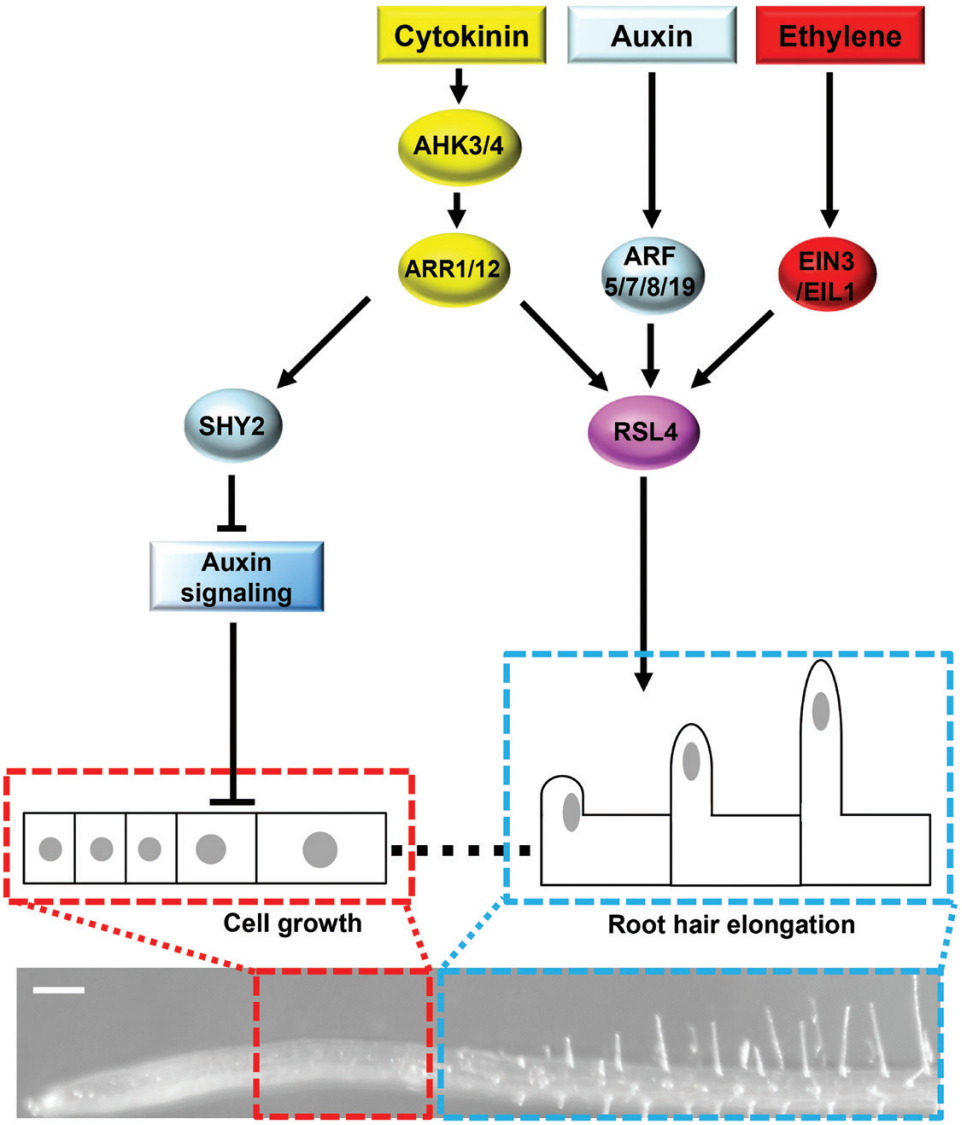

Fig. 10. CK-mediated control of cell elongation in Arabidopsis roots. The CK signal, mediated through the receptors AHK3 and AHK4 and the B-type response regulators ARR1 and ARR12, promotes active cell growth at the transition zone (red broken lines) and root hairs (blue broken lines). *SHY2*, which encodes one of the Aux/IAA family members, is up-regulated by ARR1/12, inhibiting auxin signaling and inducing cell growth at the transition zone. *RSL4* is a central regulator of root hair elongation. *RSL4* expression is directly induced by ARR1/12, ARFs, and EIN3/EIL1, the key transcription factors for cytokinin, auxin, and ethylene signaling, respectively. The scale bar represents 100 μm.

in root hair length when grown in the absence of *t*-zeatin (Fig. 2C). This suggests that ARR1 plays a predominant role in hair elongation under normal growth conditions. Choi *et al.* (2010) previously discovered interactor-based functional divergence among B-type ARRs; ARR2, but not ARR1, binds to the transcription factor TGA1A-RELATED GENE 3 (TGA3) to enhance resistance to pathogen attack. Similarly, ARR1 may have a high affinity for unknown factor(s) in H cells, thereby playing a central role in root hair elongation. However, it is also possible that distinct mRNA and/or protein levels of each B-type ARR caused different root hair phenotypes between single mutants.

A previous report demonstrated that the EIN3 protein, which accumulates in most cell types in roots, physically interacts with the H cell-specific RHD6 protein, thereby up-regulating *RSL4* expression, specifically in H cells (Feng *et al.*, 2017). A similar case was also reported for another phytohormone, jasmonate (JA), whose signaling is activated by the degradation of JAZ repressors (Chini *et al.*, 2007; Thines *et al.*, 2007; Yan *et al.*, 2009). In the absence of JA, JAZ repressors interact with the RHD6 protein and promote its degradation, consequently inhibiting root hair elongation. Upon JA perception, JAZ repressors are degraded by proteasomes and, as a result, the RHD6 protein is stabilized and enhances root hair

growth (Han *et al.*, 2020). In this study, we revealed that, in response to CK, *RSL4* is up-regulated by ARR1, specifically in H cells, while ARR1 is expressed in most cells around the transition and elongation/differentiation zones (Fig. 4A, B). It is likely that, as in the case of EIN3 and JAZ repressors, ARR1 forms a complex with H cell-specific factors, such as RHD6, thereby inducing *RSL4* only in H cells. Further studies will reveal how interacting partners give a functional and/or transcriptional specificity to ARR1 and contribute to the proper development of root hairs.

According to recent findings, controlling the magnitude of CK signaling at a whole root level is a key to environmental stress adaptation (Nguyen *et al.*, 2016; Wu *et al.*, 2021). However, regarding stress response, the role of CK in root hair growth remains controversial. Drought and salinity stresses, which suppress root hair growth, reduce the expression of B-type ARR genes, such as *ARR1* and *ARR12*, in roots (Schnall and Quatrano, 1992; Wang *et al.*, 2008; Nguyen *et al.*, 2016). In contrast, nitrogen or phosphate deficiency dramatically increases hair length but probably weakens CK signaling by decreasing CK content in roots (Robinson and Rorison, 1987; Péret *et al.*, 2011; Kamada-Nobusada *et al.*, 2013; Bhosale *et al.*, 2018; Yoneyama *et al.*, 2020). This implies that nitrogen or phosphate deficiency does not require CK signals to promote root hair elongation. There is a possibility that the signaling pathways activated by particular stresses, such as drought and salinity stresses, can inhibit root hair growth by controlling CK signals. The next question is how these pathways coordinately regulate CK signals and optimize root hair growth under fluctuating environments.

Our study revealed another input for the *RSL4* gene, namely signals of CK as well as ethylene and auxin, directly up-regulate *RSL4* expression through the distinct transcription factors, ARR1, EIN3/EIL1, and ARFs (Fig. 10). To our knowledge, there are no other examples of a single gene being directly controlled by three independent hormonal inputs, suggesting that *RSL4* offers an excellent model for understanding redundant hormonal actions to control organ growth and development. A previous study showed an additive effect of CK and ethylene on transcript accumulation; A-type *ARR* genes, *ARR3* and *ARR8*, are up-regulated by either CK or ethylene in Arabidopsis roots, while they are further induced in an additive manner upon co-treatment with the two hormones, although the physiological function remains unknown (Zdarska *et al.*, 2019). This suggests that the combination of CK, ethylene, and auxin has a bigger impact on *RSL4* transcription than the sum of each action, enabling different developmental outputs. Considering that distinct environmental signals trigger each hormonal signaling pathway, it is likely that *RSL4* functions as a core to translate various external information into root hair growth, thereby optimizing plant growth under fluctuating environments. Modifying the mechanisms underlying combinatorial regulation of *RSL4* expression may lead to the development of crops with multiple stress tolerance traits that would allow a fine-tuning of water and nutrient uptake from the soil.

Supplementary data

The following supplementary data are available at JXB online.

Fig. S1. CK affects neither cell fate nor hair initiation in the root epidermis.

Fig. S2. Expression patterns of B-type *ARR* genes in the H cell lineage.

Fig. S3. The effect of *t*-zeatin on shoot growth.

Fig. S4. *CCS52A1* or *SHY2* is not involved in CK-induced root hair elongation.

Fig. S5. Microarray data of *ARR15*, *SHY2*, and *RSL4* in the wild type and *arr1/12*.

Fig. S6. CK induces *RSL4* and enhances root hair elongation in the presence of PEO-IAA.

Table S1. List of primers used in this study.

Table S2. List of Arabidopsis genes regulated by ARR1/12.

Acknowledgements

We would like to thank Dr Liam Dolan for *pRSL4:GUS* and *rsl4-1*, and Dr Takafumi Yamashino for *arr10*.

Author contributions

MU and HT: conceptualization, and writing with contributions of all the authors; MU: supervision; HT: design and data analysis; HT and AS: performing most of the experiments; MT and MoS: performing the microarray analysis; KS and MiS: performing the ChIP-qPCR analysis; and NT performing the AlfaScreen.

Conflict of interest

The authors declare no conflict of interest.

Funding

This work was supported by MEXT KAKENHI (grant nos 17H06470, 17H06477, and 21H04715) to MU; the Core Research for Evolutionary Science and Technology (CREST; grant no. JPMJCR13B4) from the Japan Science and Technology Agency (JST) to MoS; MEXT KAKENHI (grant no. 20H05911) to KS; and MEXT KAKENHI (grant no. 22K06293), the MEXT Leading Initiative for Excellent Young Researchers, Kanazawa University JIKOCHOKOKU project, Kanazawa University SAKIGAKE project 2022, and JST PRESTO (grant no. JPMJPR22E6) to HT.

Data availability

All raw data underlying the results presented in this study are available upon request.

References

An L, Zhou Z, Sun L, *et al*. 2012. A zinc finger protein gene ZFP5 integrates phytohormone signaling to control root hair development in Arabidopsis. The Plant Journal **72**, 474–490.

Bates TR, Lynch JP. 2000. Plant growth and phosphorus accumulation of wild type and two root hair mutants of *Arabidopsis thaliana* (Brassicaceae). American Journal of Botany **87**, 958–963.

Bhosale R, Giri J, Pandey BK, *et al*. 2018. A mechanistic framework for auxin dependent Arabidopsis root hair elongation to low external phosphate. Nature Communications **9**, 1409.

Brady SM, Orlando DA, Lee JY, Wang JY, Koch J, Dinneny JR, Mace D, Ohler U, Benfey PN. 2007. A high-resolution root spatiotemporal map reveals dominant expression patterns. Science **318**, 801–806.

Cary AJ, Liu W, Howell SH. 1995. Cytokinin action is coupled to ethylene in its effects on the inhibition of root and hypocotyl elongation in *Arabidopsis thaliana* seedlings. Plant Physiology **107**, 1075–1082.

Chini A, Fonseca S, Fernández G, *et al*. 2007. The JAZ family of repressors is the missing link in jasmonate signalling. Nature **448**, 666–671.

Choi J, Huh SU, Kojima M, Sakakibara H, Paek KH, Hwang I. 2010. The cytokinin-activated transcription factor ARR2 promotes plant immunity via TGA3/NPR1-dependent salicylic acid signaling in Arabidopsis. Developmental Cell **19**, 284–295.

Dello Ioio R, Linhares FS, Scacchi E, Casamitjana-Martinez E, Heidstra R, Costantino P, Sabatini S. 2007. Cytokinins determine Arabidopsis root-meristem size by controlling cell differentiation. Current Biology **17**, 678–682.

Dello Ioio R, Nakamura K, Moubayidin L, Perilli S, Taniguchi M, Morita MT, Aoyama T, Costantino P, Sabatini S. 2008. A genetic framework for the control of cell division and differentiation in the root meristem. Science **322**, 1380–1384.

Favero DS, Kawamura A, Shibata M, *et al*. 2020. AT-hook transcription factors restrict petiole growth by antagonizing PIFs. Current Biology **30**, 1454–1466.

Feng Y, Xu P, Li B, *et al*. 2017. Ethylene promotes root hair growth through coordinated EIN3/EIL1 and RHD6/RSL1 activity in Arabidopsis. Proceedings of the National Academy of Sciences, USA **114**, 13834–13839.

Gilroy S, Jones DL. 2000. Through form to function: root hair development and nutrient uptake. Trends in Plant Science **5**, 56–60.

Guimil S, Dunand C. 2007. Cell growth and differentiation in Arabidopsis epidermal cells. Journal of Experimental Botany **58**, 3829–3840.

Han X, Zhang M, Yang M, Hu Y. 2020. Arabidopsis JAZ proteins interact with and suppress RHD6 transcription factor to regulate jasmonate-stimulated root hair development. The Plant Cell **32**, 1049–1062.

Hill K, Mathews DE, Kim HJ, *et al*. 2013. Functional characterization of type-B response regulators in the Arabidopsis cytokinin response. Plant Physiology **162**, 212–224.

Huang L, Shi X, Wang W, Ryu KH, Schiefelbein J. 2017. Diversification of root hair development genes in vascular plants. Plant Physiology **174**, 1697–1712.

Hwang I, Sheen J, Müller B. 2012. Cytokinin signaling networks. Annual Review of Plant Biology **63**, 353–380.

Inoue T, Higuchi M, Hashimoto Y, Seki M, Kobayashi M, Kato T, Tabata S, Shinozaki K, Kakimoto T. 2001. Identification of CRE1 as a cytokinin receptor from Arabidopsis. Nature **409**, 1060–1063.

Ishida T, Kurata T, Okada K, Wada T. 2008. A genetic regulatory network in the development of trichomes and root hairs. Annual Review of Plant Biology **59**, 365–386.

Jean-Baptiste K, McFaline-Figueroa JL, Alexandre CM, Dorrity MW, Saunders L, Bubb KL, Trapnell C, Fields S, Queitsch C, Cuperusa JT. 2019. Dynamics of gene expression in single root cells of *Arabidopsis thaliana*. The Plant Cell **31**, 993–1011.

Jones AR, Kramer EM, Knox K, Swarup R, Bennett MJ, Lazarus CM, Leyser HMO, Grierson CS. 2009. Auxin transport through non-hair cells sustains root-hair development. Nature Cell Biology **11**, 78–84.

Kamada-Nobusada T, Makita N, Kojima M, Sakakibara H. 2013. Nitrogen-dependent regulation of de novo cytokinin biosynthesis in rice: the role of glutamine metabolism as an additional signal. Plant and Cell Physiology **54**, 1881–1893.

Kato M, Tsuge T, Maeshima M, Aoyama T. 2019. Arabidopsis PCaP2 modulates the phosphatidylinositol 4,5-bisphosphate signal on the plasma membrane and attenuates root hair elongation. The Plant Journal **99**, 610–625.

Larson-Rabin Z, Li Z, Masson PH, Day CD. 2009. FZR2/CCS52A1 expression is a determinant of endoreduplication and cell expansion in Arabidopsis. Plant Physiology **149**, 874–884.

Le DT, Nishiyama R, Watanabe Y, Vankova R, Tanaka M, Seki M, Ham LH, Yamaguchi-Shinozaki K, Shinozaki K, Tran LSP. 2012. Identification and expression analysis of cytokinin metabolic genes in soybean under normal and drought conditions in relation to cytokinin levels. PLoS One **7**, e42411.

López-Bucio J, Cruz-Ramírez A, Herrera-Estrella L. 2003. The role of nutrient availability in regulating root architecture. Current Opinion in Plant Biology **6**, 280–287.

Mangano S, Denita-Juarez SP, Choi HS, *et al*. 2017. Molecular link between auxin and ROS-mediated polar growth. Proceedings of the National Academy of Sciences, USA **114**, 5289–5294.

Mason MG, Li J, Mathews DE, Kieber JJ, Schaller GE. 2004. Type-B response regulators display overlapping expression patterns in Arabidopsis. Plant Physiology **135**, 927–937.

Muto H, Watahiki MK, Nakamoto D, Kinjo M, Yamamoto KT. 2007. Specificity and similarity of functions of the Aux/IAA genes in auxin signaling of Arabidopsis revealed by promoter-exchange experiments among MSG2/IAA19, AXR2/IAA7, and SLR/IAA14. Plant Physiology **144**, 187–196.

Nagpal P, Walker LM, Young JC, Sonawala A, Timpte C, Estelle M, Reed JW. 2000. AXR2 encodes a member of the Aux/IAA protein family. Plant Physiology **123**, 563–574.

Nakagawa T, Kurose T, Hino T, Tanaka K, Kawamukai M, Niwa Y, Toyooka K, Matsuoka K, Jinbo T, Kimura T. 2007. Development of series of gateway binary vectors, pGWBs, for realizing efficient construction of fusion genes for plant transformation. Journal of Bioscience and Bioengineering **104**, 34–41.

Nakamura S, Mano S, Tanaka Y, *et al*. 2010. Gateway binary vectors with the bialaphos resistance gene, bar, as a selection marker for plant transformation. Bioscience, Biotechnology, and Biochemistry **74**, 1315–1319.

Nguyen KH, Ha CV, Nishiyama R, *et al*. 2016. Arabidopsis type B cytokinin response regulators ARR1, ARR10, and ARR12 negatively regulate plant responses to drought. Proceedings of the National Academy of Sciences, USA **113**, 3090–3095.

Nishimura T, Nakano H, Hayashi KI, Niwa C, Koshiba T. 2009. Differential downward stream of auxin synthesized at the tip has a key role in gravitropic curvature via TIR1/AFBS-mediated auxin signaling pathways. Plant and Cell Physiology **50**, 1874–1885.

Péret B, Clément M, Nussaume L, Desnos T. 2011. Root developmental adaptation to phosphate starvation: better safe than sorry. Trends in Plant Science **16**, 442–450.

Ramireddy E, Brenner WG, Pfeifer A, Heyl A, Schmülling T. 2013. In planta analysis of a cis-regulatory cytokinin response motif in arabidopsis and identification of a novel enhancer sequence. Plant and Cell Physiology **54**, 1079–1092.

Robinson D, Rorison IH. 1987. Root hairs and plant growth at low nitrogen availabilities. New Phytologist **107**, 681–693.

Růzička K, Šimášková M, Duclercq J, Petrášek J, Zažímalová E, Simon S, Friml J, Van Montagu MCE, Benková E. 2009. Cytokinin regulates root meristem activity via modulation of the polar auxin transport. Proceedings of the National Academy of Sciences, USA **106**, 4284–4289.

Sakai H, Honma T, Takashi A, Sato S, Kato T, Tabata S, Oka A. 2001. ARR1, a transcription factor for genes immediately responsive to cytokinins. Science **294**, 1519–1521.

Schiefelbein J, Kwak SH, Wieckowski Y, Barron C, Bruex A. 2009. The gene regulatory network for root epidermal cell-type pattern formation in Arabidopsis. Journal of Experimental Botany **60**, 1515–1521.

Schnall JA, Quatrano RS. 1992. Abscisic acid elicits the water-stress response in root hairs of *Arabidopsis thaliana*. Plant Physiology **100**, 216–218.

Shibata M, Breuer C, Kawamura A, *et al*. 2018. GTL1 and DF1 regulate root hair growth through transcriptional repression of ROOT HAIR DEFECTIVE 6-LIKE 4 in Arabidopsis. Development **145**, dev159707.

Su W, Howell SH. 1992. A single genetic locus, Ckr1, defines arabidopsis mutants in which root growth is resistant to low concentrations of cytokinin. Plant Physiology **99**, 1569–1574.

Takahashi N, Inagaki S, Nishimura K, Sakakibara H, Antoniadi I, Karady M, Ljung K, Umeda M. 2021. Alterations in hormonal signals spatially coordinate distinct responses to DNA double-strand breaks in Arabidopsis roots. Science Advances **7**, eabg0993.

Takahashi N, Kajihara T, Okamura C, Kim Y, Katagiri Y, Okushima Y, Matsunaga S, Hwang I, Umeda M. 2013. Cytokinins control endocycle onset by promoting the expression of an APC/C activator in Arabidopsis roots. Current Biology **23**, 1812–1817.

Takatsuka H, Higaki T, Umeda M. 2018. Actin reorganization triggers rapid cell elongation in roots. Plant Physiology **178**, 1130–1141.

Takatsuka H, Ito M. 2020. Cytoskeletal control of planar polarity in root hair development. Frontiers in Plant Science **11**, 1369.

Takatsuka H, Umeda M. 2019. ABA inhibits root cell elongation through repressing the cytokinin signaling. Plant Signaling and Behavior **14**, e1578632.

Taniguchi M, Sasaki N, Tsuge T, Aoyama T, Oka A. 2007. ARR1 directly activates cytokinin response genes that encode proteins with diverse regulatory functions. Plant and Cell Physiology **48**, 263–277.

Thines B, Katsir L, Melotto M, Niu Y, Mandaokar A, Liu G, Nomura K, He SY, Howe GA, Browse J. 2007. JAZ repressor proteins are targets of the SCFCOI1 complex during jasmonate signalling. Nature **448**, 661–665.

Timpte C, Wilson AK, Estelle M. 1994. The *axr2-1* mutation of *Arabidopsis thaliana* is a gain-of-function mutation that disrupts an early step in auxin response. Genetics **138**, 1239–1249.

To JPC, Haberer G, Ferreira FJ, Deruère J, Mason MG, Schaller GE, Alonso JM, Ecker JR, Kieber JJ. 2004. Type-A Arabidopsis response regulators are partially redundant negative regulators of cytokinin signaling. The Plant Cell **16**, 658–671.

To JPC, Kieber JJ. 2008. Cytokinin signaling: two-components and more. Trends in Plant Science **13**, 85–92.

Tokizawa M, Kobayashi Y, Saito T, Kobayashi M, Iuchi S, Nomoto M, Tada Y, Yamamoto YY, Koyama H. 2015. Sensitive to proton Rhizotoxicity1, calmodulin binding transcription activator2, and other transcription factors are involved in Aluminum-Activated Malate transporter1 expression. Plant Physiology **167**, 991–1003.

Wang Y, Zhang W, Li K, Sun F, Han C, Wang Y, Li X. 2008. Salt-induced plasticity of root hair development is caused by ion disequilibrium in *Arabidopsis thaliana*. Journal of Plant Research **121**, 87–96.

Wu Y, Liu H, Wang Q, Zhang G. 2021. Roles of cytokinins in root growth and abiotic stress response of *Arabidopsis thaliana*. Plant Growth Regulation **94**, 151–160.

Xie M, Chen H, Huang L, O'Neil RC, Shokhirev MN, Ecker JR. 2018. A B-ARR-mediated cytokinin transcriptional network directs hormone cross-regulation and shoot development. Nature Communications **9**, 1604.

Yamaguchi N, Winter CM, Wu M-F, Kwon CS, William DA, Wagner D. 2014. Protocols: chromatin immunoprecipitation from arabidopsis tissues. The Arabidopsis Book **12**, e0170.

Yan J, Zhang C, Gu M, *et al*. 2009. The arabidopsis CORONATINE INSENSITIVE1 protein is a jasmonate receptor. The Plant Cell **21**, 2220–2236.

Yi K, Menand B, Bell E, Dolan L. 2010. A basic helix–loop–helix transcription factor controls cell growth and size in root hairs. Nature Genetics **42**, 264–267.

Yoneyama K, Xie X, Nomura T, Yoneyama K. 2020. Do phosphate and cytokinin interact to regulate strigolactone biosynthesis or act independently? Frontiers in Plant Science **11**, 438.

Zdarska M, Cuyacot AR, Tarr PT, Yamoune A, Szmitkowska A, Hrdinová V, Gelová Z, Meyerowitz EM, Hejátko J. 2019. ETR1 integrates response to ethylene and cytokinins into a single multistep phosphorelay pathway to control root growth. Molecular Plant **12**, 1338–1352.

Zhang S, Huang L, Yan A, Liu Y, Liu B, Yu C, Zhang A, Schiefelbein J, Gan Y. 2016. Multiple phytohormones promote root hair elongation by regulating a similar set of genes in the root epidermis in Arabidopsis. Journal of Experimental Botany **67**, 6363–6372.